14th Czech.Sem. on Plasma Phys. and Techn., Liblice 1987

FAST IONS BEHAVIOUR ON THE CASTOR TOKAMAK DURING THE LOW DENSITY DISCHARGE WITH COMBINED INDUCTIVE AND LOWER HYBRID CURRENT DRIVE

Petrov S.

Physico-Technical Institute A. F. Ioffe, Leningrad

Stöckel J., Jakubka K., Valovič M., Žáček F., Badalec J.

Institute of Plasma Physics, Czechoslovak Academy of Sciences
Prague

Experimental arrangement: Preliminary results concerning with fast ions behaviour on the CASTOR tokamak during the low density inductive and combined inductive-lower hybrid current drive (LHCD) are reported. The investigated regimes can be characterized by rather low density ($n_e \lesssim 6.10^{18}$ m^{-3}) and plasma current ($J_p < 10$ kA) as consequence of relatively low pumping frequency (f = 1.24 GHz) and power level (P_{RF} = 40 kW) of the RF-generator. Just under such conditions, the LHCD-effects are well expressed in our case.

Parameters of the CASTOR tokamak (R = 0.4 m, a = 0.085 m, B_T = 1.3 T) and RF-launcher (the 4-waveguide multijunction grill) have already been described elswere in more details /1/. The experimental arrangement is schematically illustrated in Fig. 1. The RF-impulse is usually switched on at t $\gtrsim$ 2.5 ms after start of the ohmical heating (OH) tokamak discharge, when the stationary phase of the discharge is already established. The OH-system continues in operation during the RF--power application, therefore, the investigated regime can be characterized as a combined inductive and RF-current drive /2/. The fast ions behaviour (E > 100 eV) is deduced from energy spectra of energetic neutral hydrogen atoms, measured by the five channel neutral particle analyzer /3/ with a new data aquisition system /4/ allowing to obtain the time evolution of the neutral fluxes during the whole discharge with the temporal resolution 0.1 - 1 ms. Each point of the energy spectrum is averaged over 3 - 5 shots due to the rather low statistics.

Inductive current drive (OH target plasma): An example of time evolution of some basic parameters of the low density OH discharge is depicted in Fig. 2. The low density regime can be achieved just after carefull cleaning of the liner and without using any impulse gas puffing. Then the line average plasma density decreases exponentially from its maximum value at T = 0.7 ms with a time constant $\tau_{\bar{n}e} \simeq$ 3 - 4 ms. During the stationary phase of the discharge, the radiative power losses are relatively unimportant with respect to the OH-power input ($P_{RAD}/P_{OH} \simeq 0.3$). The electron temperature estimated from Spitzer conductivity is non-classical and most probably, a substantial number of overthermal electrons is present in the discharge.

A characteristic feature of the described regime is an instability, which is rutinely observed when the plasma density falls to the value $\bar{n}_e = 2 - 3.10^{18} m^{-3}$. This instability is manifested by:

a) a positive spike on the loop voltage,

b) a fast inward displacement of the plasma column. The major radius of the plasma column drops from ~ 45 mm to ~ 35 mm, probably due to the decrease of the internal energy of the plasma,

c) a very intensive burst of the microwave radiation in the range of electron cyclotron resonance,

d) a sharp peak of the hard X-ray emission (E > 150 keV),

e) sometimes a step increase of the radiated power P_{RAD}.

There are no noticable changes either on the plasma current or on the line average density.

According to the phenomenological description, the instability can be classified as the anisotropy-driven (or fan-like) instability. This phenomenon leads to the fast (non-collisional) isotropization of the previously anisotropic electron distribution function. The similar effect has been already observed earlier on the TM-3 /5/ and TFR /6/ tokamaks and discussed in /7/.

Behaviour of the ion component during the low density discharge is noticeably influenced by the presence of the instability. It is documented in Fig. 3, which presents the temporal evolution of neutral particle fluxes at energies 0.1 - 1.4 keV with time resolution $\Delta t = 1$ ms. The instability takes place at $t = 4$ ms in this case. A step increase of the fluxes with energies above $E \simeq 350$ eV is evident. It is interesting to note that the increase takes place not only during the instability but persists until the end of the discharge. It is in contrast with former charge-exchange measurements on TM-3 tokamak /5/, where only short spike of the high energy atoms has been observed just during the instability.

Energy spectra of the fast neutrals, recalculated from the neutral fluxes are depicted in Fig. 4. Before the instability ($\bar{n}_e > 3.10^{18}$ m^{-3}), the low energy part of the spectral has a slope of about 30 eV while the high energy part ($E > 200$ eV) has a slope approx. two times greater. The question, what part of the experimental spectrum corresponds to the bulk of the ion distribution function has to be solved later by one of us (S.P.) by comparison of the experimental neutral fluxes with a numerical simulation of them in the mentioned regime. Nevertheless, before that we can suppose that the low energy part of the spectrum corresponds to the periphery while the high energy part describes the hot central region of the plasma column. The determined central ion temperature $T_i(0) = 50$ eV before instability agrees well with the Artsimovitch formula, derived under stationary conditions, assuming a classical electron-ion coupling as a power input to the ion component. However, taking into account rather short time interval from the beginning of the discharge (~ 3 ms) and long enough characteristic time for the electron-ion temperature equilibration ($\tau_{ei}^{E} > 10$ ms), the equilibrium cannot be reached and some non-classical mechanism of ion heating should take place.

The anomalous ion heating is much more expressed during and after the fan-like instability. The part of the spectrum describing the hot plasma core lays probably between 150 and 500 eV and it has the slope of about 150 eV, which is well above the Artsimovitch estimate. Moreover, the high energy tails with a slope ~ 300 eV are registered. According to the review paper [7], the dominant mechanism of the anomalous ion heating during the fanlike instability seems to be a nonlinear scattering of Langmuir waves on plasma ions. The Langmuir plasmons are created due to the anomalous Doppler effect. Generation of the microwave radiation is manifested experimentally by the intensive short burst at the wavelength around $\lambda = 8$ mm, registered by the broad band detector outside the plasma column. However, it should be pointed once more that, in our case, the anomalous heating is observed not only during the instability but it takes place also later on at times long enough with respect to the energy confinement time, when all macroscopic parameters indicate a "stable" discharge.

Combined inductive and LH current drive: The RF-power is applied at $\bar{n}_e = 6.10^{18}\ m^{-3}$ i.e. at t = 3 ms. The time evolution of the loop voltage during combined inductive/RF current drive, typical for the described experimental series, is shown in Fig. 5. Unfortunately, we were not able to realize a stable regime during the whole RF power application. An initial stable decrease of the loop voltage $\Delta\ U/U = 0.55$ indicates that of about ~ 5 kA of the plasma current is driven by LH waves at the end of this phase. It is followed by an unstable period with characteristic positive spikes on the loop voltage, which suggests the anomalous Doppler mode like in the pure OH discharge. The similar periodical behaviour is shown by other diagnostics (hard X-ray monitor, ECE-detector, magnetic probes) as well. However, it should be pointed out that these periodical anomalous Doppler modes appear at higher densities and, the bursts of the EC emission are not so expressed as in the pure inductive discharge. The question, how to control the stability of the LHCD with respect to the anomalous Doppler mode is still open in our case. Nevertheless, there are some indications that the stability can be influenced by the concentration of impurities. Usually, the stable regime is reached after sufficiently long tokamak operation without opening of the liner to the atmosphere. In the case shown, the unstable period is followed by the stable phase but with substantially lower efficiency of LHCD.

The neutral fluxes during the inductive/LH current drive can be characterized by a noticeable scattering of the experimental data, especially during the unstable period of the current drive. An example of the time evolution of the neutral fluxes (Fig. 5) shows their substantial increase during the unstable period. However, in contrary to the OH discharge, this enhancement is deteriorated when the discharge is further stabilized. The energy spectra (Fig. 6) during the first stable period exhibit high energy tails with a slope ~300 eV. But, according to rough estimates, these high energy atoms play only uniportant role in the global or particle balance during the combined inductive/LH current drive. Practically the same tails appear in the energy spectra after the unstable period. Large scattering of the experimental data during the periodical instabilities don´t allow to estimate any slope of the energy spectrum. However, by comparing with the inductive discharge, the experimental points lay roughly around the slope determined during and after the fan-like instability.

References

/1/ Nanobashvili S., Ďatlov J., Stöckel J., Žáček F.: Czech. J. Phys., B 37, 1987, p. 194.
/2/ Stöckel J., Žáček F.: Czech. J. Phys., B 37, 1987, p. 201.
/3/ Afrosimov V. V. et al.: Zh. tech. fyz., 45, 1975, 35.
/4/ Petrov S., Stöckel J.: to be published as Int. Rep. ÚFP ČSAV
/5/ Alikaev V. V., Razumova K. A., Sokolov Ju. A.: Fyzika plazmy 1, 1975, 546.

[6] TFR group: Nucl. Fus., 16, 1976, p. 473.
[7] Parail V. V., Pogutse O. P.: Voprosy teorii plazmy, Vol. 11 Energoizdat, Moscow, 1982.

Figure captions:

Fig. 1 Experimental arrangement

Fig. 2 Time evolution of the low density CASTOR discharge

Fig. 3 Evolution of the neutral particle fluxes for inductive current drive

Fig. 4 Energy spectra of the charge-exchange atoms (inductive current drive)

Fig. 5 Evolution of the neutral particle fluxes for combined inductive/LH current drive
Temporal evolution of the loop voltage for the same regime. I. stable period
II. unstable anomalous Doppler modes
III. stable period - low efficiency of LHCD

Fig. 6 Energy spectra of charge-exchange atoms for combined inductive/LH current drive

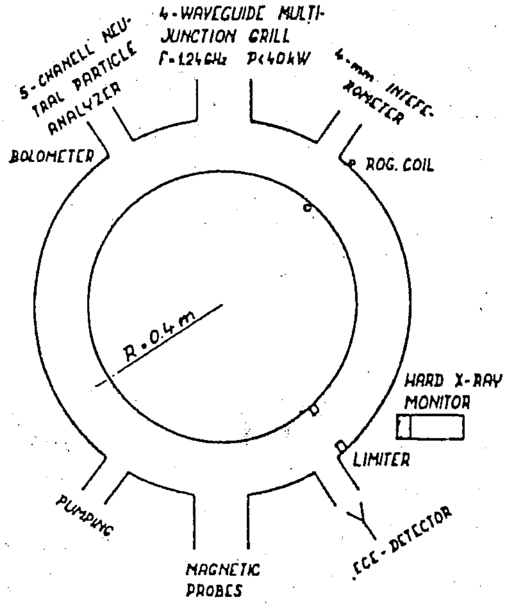

Fig. 1

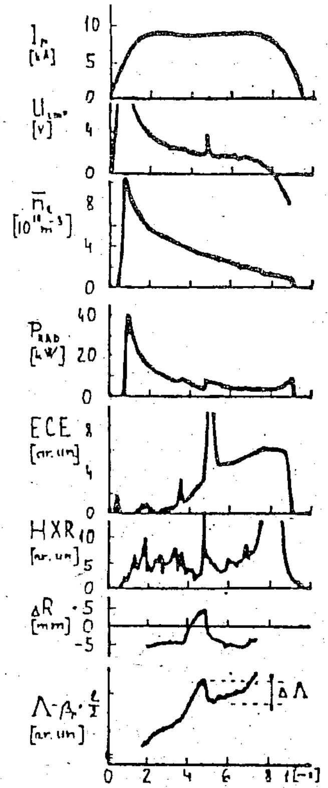

Fig. 2

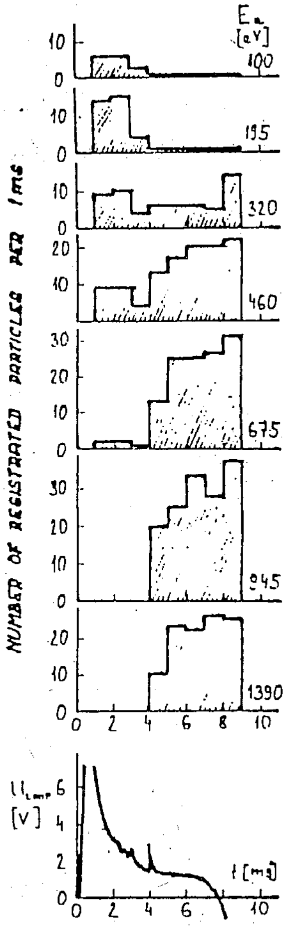

Fig. 3

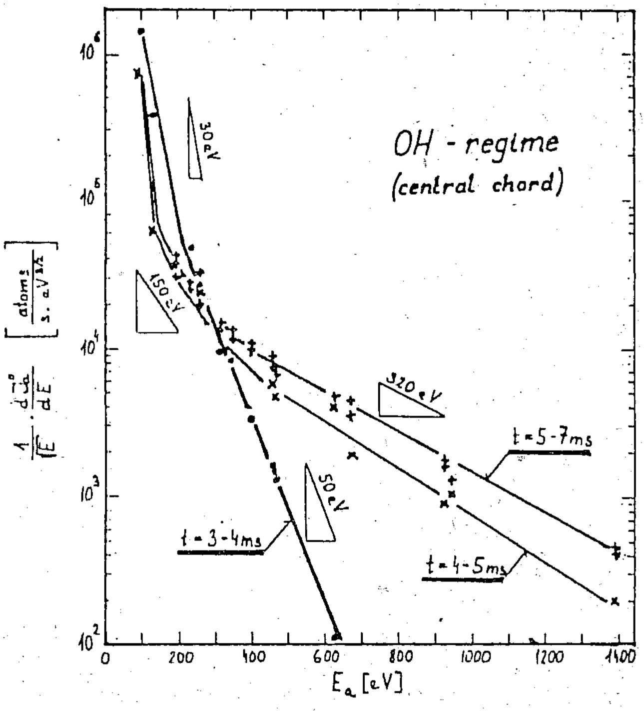

Fig. 4

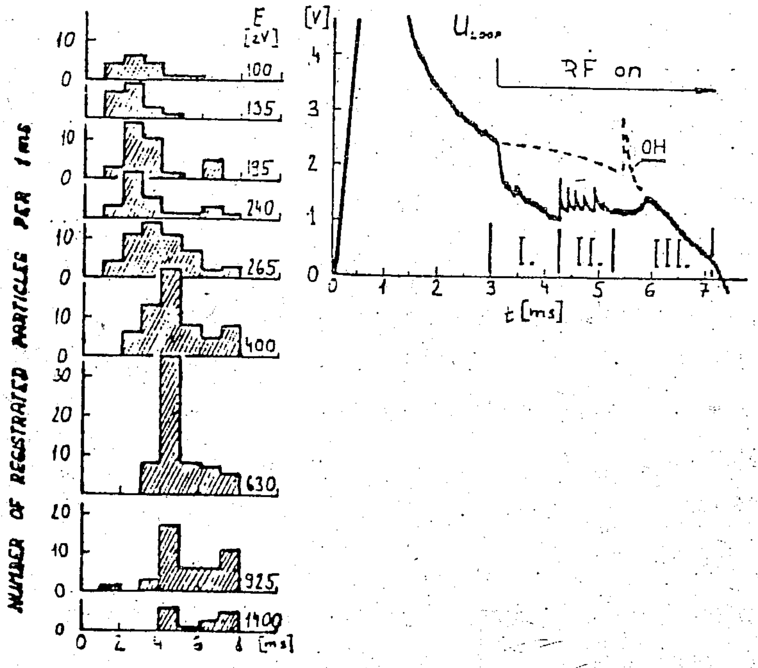
NUMBER OF REGISTRATED PARTICLES PER 1ms
E [eV]
100
135
195
240
265
400
630
925
1400
0
10
20
30
0 2 4 6 8 [ms]
[V]
U_Loop
RF on
OH
I.
II.
III.
0 1 2 3 4
0 1 2 3 4 5 6 7
t [ms]

Fig. 5

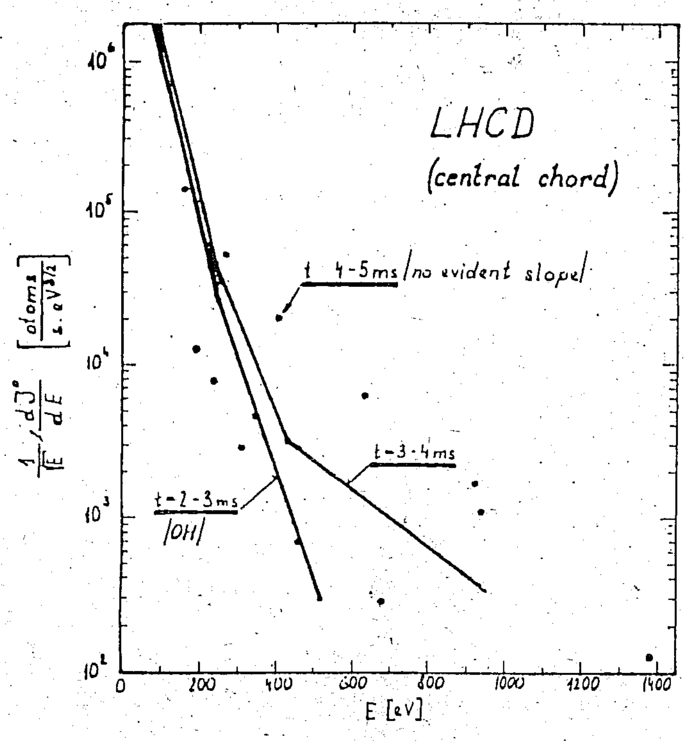
LHCD
(central chord)
t 4-5ms /no evident slope/
t=3-4ms
t=2-3ms
/OH/
$\frac{1}{\sqrt{E}} \frac{dJ^{\circ}}{dE}$ $\left[\frac{atoms}{s \cdot eV^{3/2}}\right]$
10^2
10^3
10^4
10^5
10^6
0 200 400 600 800 1000 1200 1400
E [eV]

Fig. 6